# A STUDY OF THE MODAL STRAIN ENERGY METHOD FOR VISCOELASTICALLY DAMPED STRUCTURES

Meng-Hao Tsai* and Kuo-Chun Chang
*Department of Civil Engineering*
*National Taiwan University*
*Taipei, Taiwan 106, R.O.C.*

***Key Words:*** modal strain energy, modal damping ratio, viscoelastic damper.

## ABSTRACT

The modal strain energy (MSE) method has been proposed to estimate the modal loss factors or modal damping ratios of structures with viscoelastic dampers. There are certain assumptions made in deriving the MSE method, such as the computation of the modal loss factor directly from the ratios of the imaginary and real parts of the eigenvalues, and the neglect of the influence of the imaginary mode shapes, etc. These assumptions may result in overestimating the modal damping ratios of viscoelastically damped structures when the added damping is high. In this study, the effect of the assumptions made by the MSE method is investigated, and modified formulations of the MSE method are derived. The modified MSE method removes the assumptions made in the original MSE method. Furthermore, earthquake responses of a complex stiffness system and a linear viscous damping system, of which the modal damping ratios are estimated by the MSE method, are compared. Study results indicate that the difference arising from the assumptions becomes significant when the damping ratio is larger than 20%. For the illustrated non-proportionally damped system, the effect of imaginary mode shapes on the MSE method can be neglected when the damping ratio is smaller than 20%. It is then concluded that, for most engineering applications with design damping ratios smaller than 20%, the conventional linear viscous damping model with the MSE method may result in solutions in good agreement with those obtained by the more rigorous complex stiffness model.

## I. INTRODUCTION

Viscoelastic (VE) dampers have been shown to be effective energy dissipators for seismic structural applications. Since VE dampers are used for providing extra damping to the structures, the composite damping ratio of viscoelastically damped structures is one of the key parameters to be determined for dynamic analyses. The modal strain energy (MSE) method has been proposed to estimate the modal loss factors or modal damping ratios of structures with VE dampers (Johnson and Kienholz 1982). The accuracy of the MSE method has been demonstrated through experimental studies (Chang *et al*. 1995) on model structures, as shown in Fig. 1, and analytical studies on the exact and approximate mean-square

*Correspondence addressee

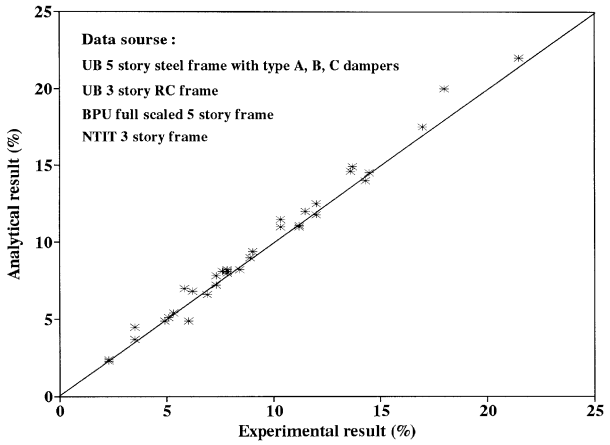


Fig. 1 Comparison of modal damping ratios obtained by the MSE method and test results

responses of structures with added VE dampers (Zambrano *et al*. 1996). In addition, experimental studies and the corresponding numerical analyses have indicated that the linear viscous damping model incorporated with the MSE method can precisely predict the dynamic response of viscoelastically damped steel frames (Chang *et al*. 1995). In earthquake resistant applications, the MSE method has also been applied to design structures with added VE dampers (Chang *et al*.1998a, Shen *et al*.1995).

However, the MSE method used to estimate the damping ratio of the linear viscous damping model is derived from the eigenvalue analysis of a complex stiffness model. Consequently, there are some assumptions made in the original derivation, such as the computation of the modal loss factor directly from the ratio of the imaginary and real part of the eigenvalue, and the neglect of the influence of imaginary mode shapes, etc. These assumptions may result in overestimating the modal damping ratios of viscoelastically damped structures when the added damping is high. In this study, the effect of such assumptions on the predicted modal damping ratio is investigated, and modified MSE methods are derived. The modified MSE methods suggest a range of applications where the original MSE method may apply for modal damping ratio prediction. Moreover, seismic responses of a complex stiffness system and a linear viscous damping system, of which modal damping ratios are estimated by the MSE method, are compared to illustrate the difference.

## II. MODAL STRAIN ENERGY METHOD

### 1. Practical Formulation (MSE1)

The differential equation of a complex stiffness system under free vibration in the frequency domain is expressed as (Johnson and Kienholz 1982)

$$\boldsymbol{M}\ddot{\boldsymbol{X}}(j\omega)+(\boldsymbol{K}_1+j\boldsymbol{K}_2)\boldsymbol{X}(j\omega)=0 \tag{1}$$

where $\boldsymbol{M}$ is the mass matrix; $\boldsymbol{K}_1$ and $\boldsymbol{K}_2$ are the elastic and loss stiffness matrices of the system, respectively; $j=\sqrt{-1}$, and $\boldsymbol{X}$ is the displacement vector in the frequency domain. Eq. (1) can be converted to an eigenvalue problem as:

$$(\boldsymbol{K}_1+j\boldsymbol{K}_2)\phi_i^* = \lambda_i^{*2}\boldsymbol{M}\phi_i^* \tag{2}$$

where $\phi_i^*$ and $\lambda_i^{*2}$ are the $i$-th complex mode shape and eigenvalue, respectively. If the modal index $i$ is dropped for convenience, $\lambda_i^{*2}$ is expressed as

$$\lambda^{*2}=\lambda^2(1+j\eta) \tag{3}$$

Furthermore, if $\phi^*$ is approximated by a real mode shape $\phi_R$, which is obtained from the eigenvalue analysis by neglecting the loss stiffness $K_2$, and $\phi_R^T$ is pre-multiplied on both sides of Eq. (2), $\lambda^2(1+j\eta)$ is written as

$$\lambda^2(1+j\eta)=\frac{\phi_R^T\boldsymbol{K}_1\phi_R}{\phi_R^T\boldsymbol{M}\phi_R}+j\frac{\phi_R^T\boldsymbol{K}_2\phi_R}{\phi_R^T\boldsymbol{M}\phi_R} \tag{4}$$

Equating the real part and imaginary part of Eq. (4) gives

$$\lambda^2=\frac{\phi_R^T\boldsymbol{K}_1\phi_R}{\phi_R^T\boldsymbol{M}\phi_R} \tag{5}$$

and

$$\eta=\frac{\phi_R^T\boldsymbol{K}_2\phi_R}{\phi_R^T\boldsymbol{M}\phi_R}. \tag{6}$$

The value of $\lambda$ obtained from Eq. (6) is the undamped modal frequency based on the real part of the stiffness matrix. Note that $\boldsymbol{K}_2$ is the loss stiffness contributed by the added VE dampers only, and $\boldsymbol{K}_1$ is the composite stiffness composed of the storage stiffness of the VE dampers and the elastic stiffness of the primary system, which is defined as the structural system without VE dampers. Therefore, $\boldsymbol{K}_2$ and $\boldsymbol{K}_1$ can be expressed as

$$\boldsymbol{K}_2=\boldsymbol{K}_{VI} \quad \text{and} \quad \boldsymbol{K}_1=\boldsymbol{K}_{VR}+\boldsymbol{K}_0 \tag{7, 8}$$

where $\boldsymbol{K}_{VI}$ and $\boldsymbol{K}_{VR}$ are the loss stiffness and storage stiffness provided by the dampers, respectively; $\boldsymbol{K}_0$ is the elastic stiffness of the primary system. Furthermore, if all dampers have the same loss factor, $\eta_v$, then

$$\boldsymbol{K}_2=\eta_v\boldsymbol{K}_{VR} \tag{9}$$

Combining Eqs. (6), (7), (8) and (9) results in

$$\eta=\eta_v\frac{\phi_R^T\boldsymbol{K}_{VR}\phi_R}{\phi_R^T(\boldsymbol{K}_{VR}+\boldsymbol{K}_0)\phi_R} \tag{10}$$

where $\phi_R^T\boldsymbol{K}_{VR}\phi_R$ is the modal strain energy contributed by the VE dampers and $\phi_R^T(\boldsymbol{K}_{VR}+\boldsymbol{K}_0)\phi_R$ is the total modal strain energy. The value of $\eta$ obtained from Eq. (6) or Eq. (10) is the so-called modal loss factor (Johnson and Kienholz 1982), and the modal damping ratio $\xi$ is equal to $\eta/2$. Moreover, it is easy to prove that the usual adoption of $\boldsymbol{Ceq}=\boldsymbol{K}_2/\lambda$ for the damping matrix leads to the same modal loss factor as expected by the MSE1 method.

## 2. Proportionally Damped System (MSE2)

Although the MSE1 method is derived from the characteristic equation of a complex stiffness system, the modal damping ratio obtained is an approximation due to the definition of $\eta$ in Eq. (3). Alternatively, the square root of the eigenvalue, $\lambda^*$, in Eq. (3) can be expressed as

$$\lambda^*=\alpha+j\beta \tag{11}$$

According to the theory of structural dynamics, the real part and imaginary part of $\lambda^*$ are related to the modal damping ratio $\xi$ and undamped modal frequency $\omega_n$ as

$$\alpha=\omega_n\sqrt{1-\xi^2} \quad \text{and} \quad \beta=\omega_n\xi \tag{12, 13}$$

Also, from Eq.(3), it is seen that $\alpha$ and $\beta$ are the real and imaginary parts of $\lambda\sqrt{1+j\eta}$, which can be expressed as

$$\lambda\sqrt{1+j\eta}=\lambda(1+\eta^2)^{1/4}e^{j\delta/2} \tag{14}$$

$$\text{where } \tan\delta=\eta,\ \cos(\delta/2)=\frac{1}{\sqrt{2}}\left(\frac{\sqrt{1+\eta^2}+1}{\sqrt{1+\eta^2}}\right)^{1/2} \tag{15, 16}$$

$$\text{and } \sin(\delta/2)=\frac{1}{\sqrt{2}}\left(\frac{\sqrt{1+\eta^2}-1}{\sqrt{1+\eta^2}}\right)^{1/2}. \tag{17}$$

Substituting Eqs. (15), (16) and (17) into Eq.(14), $\alpha+j\beta$ can be further written as

$$\alpha+j\beta=\lambda\sqrt{1+j\eta}=\frac{\lambda}{\sqrt{2}}\{(\sqrt{1+\eta^2}+1)^{1/2}+j(\sqrt{1+\eta^2}-1)^{1/2}\} \tag{18}$$

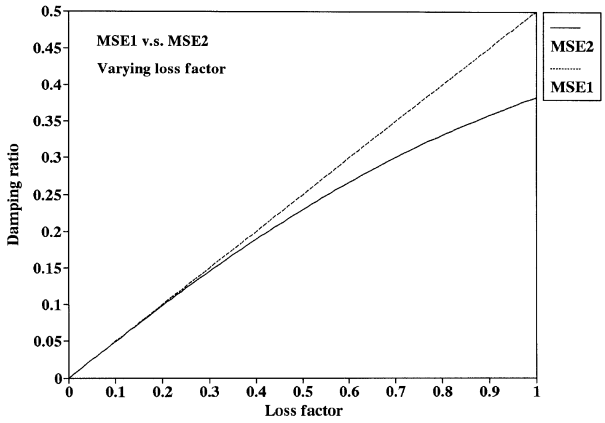


Fig. 2 Modal damping ratios estimated by the MSE1 and MSE2 methods for various loss factors

Since

$$\frac{\alpha^2}{\beta^2}=\frac{1-\xi^2}{\xi^2} \tag{19}$$

the modal damping ratio $\xi$ can be determined from

$$\frac{1-\xi^2}{\xi^2}=\frac{\sqrt{1+\eta^2}+1}{\sqrt{1+\eta^2}-1}. \tag{20}$$

The final result gives

$$=\left[\frac{1}{2}\left(1-\frac{1}{\sqrt{1+\eta^2}}\right)\right]^{1/2} \tag{21}$$

This modal damping ratio is obtained from the square root of the eigenvalue of a complex stiffness system. The value of $\eta$ in the above equation is the same as that in Eq. (6), in which the assumption of proportional damping is implied.

The modal damping ratios calculated from Eq. (21) with various loss factors, $\eta$, which is based on the MSE1 method, are shown in Fig. 2. It is obvious that the difference becomes significant as the modal damping ratio obtained from the MSE1 method increases. As seen in the figure, both methods give almost identical values when the modal damping ratio is smaller than 20%. However, when the modal damping ratios expected by the MSE1 method increase to 30% and 40%, the corresponding values obtained by the modified method (MSE2) are 26% and 33%, respectively. Alternatively, when the variation of the stiffness ratio (the ratio of the storage stiffness of dampers to the elastic stiffness of the primary structure) is considered, the difference in the predicted modal damping ratio is shown in Fig. 3 based

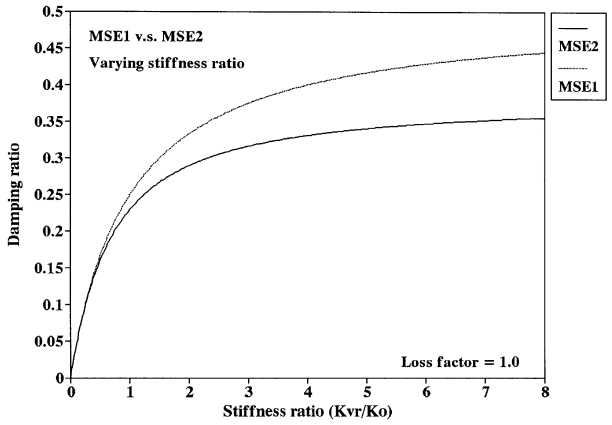


Fig. 3 Modal damping ratios estimated by the MSE1 and MSE2 methods for various stiffness ratios

on a damper loss factor $\eta_v$=1. In Fig. 3, it is realized that increasing the stiffness ratio will enhance the contribution of VE dampers to the modal damping ratio. Furthermore, the MSE1 method predicts larger modal damping ratios than the MSE2 method does under the same stiffness ratio, especially when the stiffness ratios are larger than 1.0. The difference in the predicted modal damping ratios increases gradually as the stiffness ratio increases.

### 3. Non-proportionally Damped System (MSE3)

The previous formulations are based on a proportionally damped system and thus neglect the effect of imaginary mode shapes. Since a multiple degrees-of-freedom (MDOF) structure may be non-proportionally damped, it is necessary to investigate the effect of imaginary mode shapes on the MSE1 method. For non-proportionally damped systems, the derivation of $\eta$ may proceed without suppressing the imaginary mode shapes as follows.

Pre-multiplying $\phi^{*T}$ on both sides of Eq. (2) and dropping the modal index $i$, it becomes

$$\phi^{*T}(\boldsymbol{K}_1 + \boldsymbol{j}\boldsymbol{K}_2)\phi^* = \lambda^{*2}\phi^{*T}\boldsymbol{M}\phi^* \tag{22}$$

where $\phi^{*T}$ is the conjugate transpose row vector of $\phi^*$. $\phi^*$ can be expressed as

$$\phi^* = \phi_R + j\phi_I \tag{23}$$

where $\phi_R$ and $\phi_I$ are the real and imaginary part of the complex mode shape, respectively. Substituting Eqs. (3) and (23) into Eq. (22), it yields

$$(\phi_R^T\boldsymbol{K}_1\phi_R + \phi_I^T\boldsymbol{K}_1\phi_I) + \boldsymbol{j}(\phi_R^T\boldsymbol{K}_2\phi_R + \phi_I^T\boldsymbol{K}_2\phi_I)$$
$$= \lambda^2(1 + \boldsymbol{j}\eta)(\phi_R^T\boldsymbol{M}\phi_R + \phi_I^T\boldsymbol{M}\phi_I) \tag{24}$$

Since the matrices of $\boldsymbol{K}_1$, $\boldsymbol{K}_2$, and $\boldsymbol{M}$ are symmetric, the following relations of equality are used in Eq. (24):

$$\phi_R^T\boldsymbol{K}_1\phi_I = \phi_I^T\boldsymbol{K}_1\phi_R,\ \ \phi_R^T\boldsymbol{K}_2\phi_I = \phi_I^T\boldsymbol{K}_2\phi_R,$$
$$\phi_R^T\boldsymbol{M}\phi_I = \phi_I^T\boldsymbol{M}\phi_R \tag{25, 26, 27}$$

In a way similar to Eqs. (4)~(6), the modal loss factor, $\eta$, can be estimated by

$$\eta = \frac{\phi_R^T\boldsymbol{K}_2\phi_R + \phi_I^T\boldsymbol{K}_2\phi_I}{\phi_R^T\boldsymbol{K}_1\phi_R + \phi_I^T\boldsymbol{K}_1\phi_I} \tag{28}$$

It is clear that the contribution of the imaginary mode shape depends on the value of $(\phi_I^T\phi_I)/(\phi_R^T\phi_R)$, which can be used as a measure of non-proportionality of damping in a system. Now, the value of $\eta$ determined by Eq. (28) has taken the complex mode shapes into account, and the modal damping ratio obtained from the characteristic equation can be determined by substituting $\eta$ into Eq. (21).

The effect of imaginary mode shapes on the MSE1 method is illustrated by a shear-type, 2DOF model with added VE dampers in this study. The mode shape of this system can be written as

$$\phi^* = \begin{Bmatrix} 1 \\ \phi_{1r} \end{Bmatrix} + \boldsymbol{j}\begin{Bmatrix} 1 \\ \phi_{1i} \end{Bmatrix} \tag{29}$$

in which the amplitude of the top floor is set to 1, and $\phi_{1r}$, $\phi_{1i}$ are the real and imaginary part of the modal amplitude at the first floor, respectively. Substituting Eq. (29) into Eq. (28), the modal loss factor becomes

$$\eta = \frac{k_1''\phi_{1r}^2 + k_2''(1-\phi_{1r})^2 + (k_1'' + k_2'')\phi_{1i}^2}{k_1'\phi_{1r}^2 + k_2'(1-\phi_{1r})^2 + (k_1' + k_2')\phi_{1i}^2} \tag{30}$$

in which $k_1'$ and $k_1''$ are the storage and loss stiffness of the bottom story, respectively, while $k_2'$ and $k_2''$ are those of the top story. For the story without VE dampers, the loss stiffness of the story represents the inherent damping of it. Eq. (30) indicates that the value of $\phi_{1i}^2/\phi_{1r}^2$ determines the contribution of imaginary mode shapes to the modal loss factor estimated by the MSE1 method.

The mass and elastic stiffness ratios are, respectively, defined as

$$\gamma = m_2/m_1 \text{ and } R_s = k_2'/k_1' \tag{31, 32}$$

where $m_1$ and $m_2$ are the floor mass of the bottom and

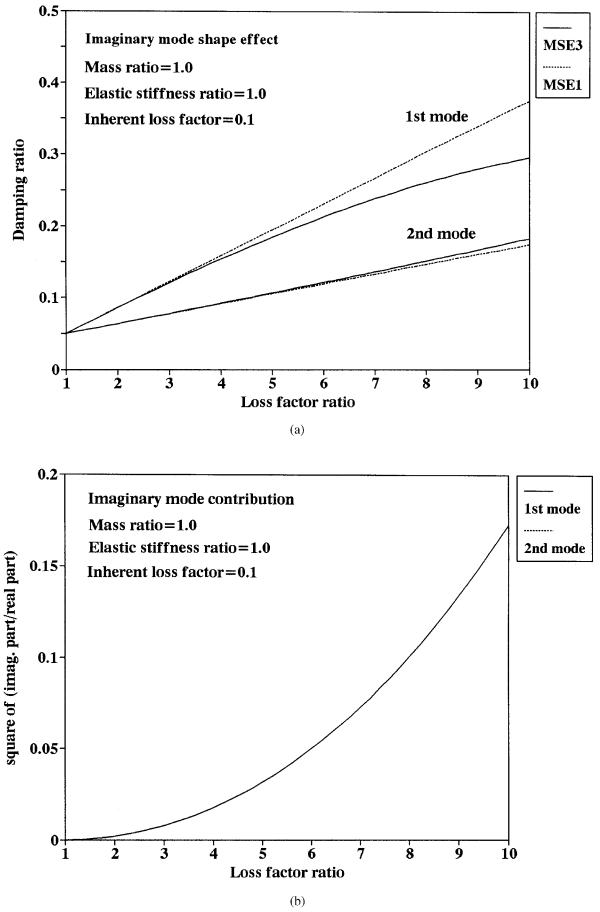


Fig. 4 (a) Modal damping ratios obtained by the MSE1 and MSE3 methods (Non-proportional 2DOF system); (b) Imaginary mode shape contribution : variation of $\phi_{1i}^2/\phi_{1ir}^2$ (Non-proportional 2DOF system)

the top story, respectively. The modal damping ratios of this system can be calculated based on specified values of $\gamma$, $R_s$, and the loss factor of each story. An extreme case is considered that the VE dampers are installed in the bottom story only. Let both the mass and elastic stiffness ratios are equal to 1.0 and the top story has an inherent loss factor, denoted by $\eta_2$, equal to 0.1. The influence of imaginary mode shapes on the MSE1 method can be examined by increasing the loss factor of the bottom story, denoted by $\eta_1$, from 0.1 to 1.0. The modal damping ratios, estimated by Eqs. (6) and (28), are compared in Fig. 4(a). Similar to the proportionally damped system, the difference of the 1st modal damping ratio increases significantly when it is larger than 20%. The variation of $\phi_{1i}^2/\phi_{1r}^2$ with increasing $\eta_1$ is shown in Fig. 4(b). It is seen that as the ratio of $\eta_1/\eta_2$ increases, the value of $\phi_{1i}^2/\phi_{1r}^2$ increases. Furthermore, since the 2nd modal damping ratios are small compared to the 1st modal damping ratios, the difference is not significant even under the condition of maximum $\eta_1/\eta_2$ value, as seen in Fig. 4(a). Hence, the imaginary mode shape will affect the results predicted by the MSE1 method only when both the modal damping ratio and $\phi_{1i}^2/\phi_{1r}^2$ are large.

## III. STRUCTURAL RESPONSE ANALYSIS

### 1. Linear Viscous Damping Model vs. Complex Stiffness Model

If the complex stiffness system is subjected to ground acceleration, the equation of motion is described by

$$\boldsymbol{M}\ddot{\boldsymbol{X}}(j\omega)+(\boldsymbol{K}_1+j\boldsymbol{K}_2)\boldsymbol{X}(j\omega)=-\boldsymbol{M}\ddot{\boldsymbol{X}}_g(j\omega) \tag{33}$$

or by an alternative form (Myklestad 1952)

$$\boldsymbol{M}\ddot{\boldsymbol{X}}(j\omega)+\boldsymbol{K}e^{j2\theta}\boldsymbol{X}(j\omega)=-\boldsymbol{M}\ddot{\boldsymbol{X}}_g(j\omega) \tag{34}$$

where $\ddot{\boldsymbol{X}}_g(j\omega)$ is the Fourier transform of the input acceleration, $2\theta$ is the phase angle between the force and displacement, and $\boldsymbol{K}$ is equal to the maximum force divided by the maximum displacement. Accordingly, for a single degree-of-freedom (SDOF) complex stiffness system, the undamped natural frequency of the complex stiffness system is written as

$$\omega_d=\lambda(1+\eta^2)^{1/4}=\sqrt{\frac{k_1}{m}}(1+\eta^2)^{1/4}=\sqrt{k/m} \tag{35}$$

It can also be derived by performing $\sqrt{\alpha^2+\beta^2}$, where $\alpha$ and $\beta$ can be found in Eq. (18). Recall that

$$\lambda=\sqrt{k_1/m} \tag{36}$$

is the undamped natural frequency of the complex stiffness system in the derivation of the MSE1 method. Hence, the value of $\lambda$ is equal to $\omega_d$ (Eq. (24a)) only when the value of $\eta$ is small.

Moreover, when the input acceleration is harmonic excitation, the magnitude of $X(j\omega)$ and $\ddot{\boldsymbol{X}}_a(j\omega)$, and the phase angle of $X(j\omega)$ are derived as

$$\left|\boldsymbol{X}(j\omega)\right|=\frac{1}{\omega_n^2\sqrt{(1-\beta_\omega^2)^2+4\beta_\omega^2\xi^2}} \tag{37}$$

$$\left|\ddot{\boldsymbol{X}}_a(j\omega)\right|=\frac{1}{\sqrt{(1-\beta_\omega^2)^2+4\beta_\omega^2\xi^2}} \tag{38}$$

$$\text{and } \angle\boldsymbol{X}(j\omega)=\tan^{-1}\frac{\eta}{1-\beta_\omega^2\sqrt{1+\eta^2}} \tag{39}$$

where $\xi$ is expressed by Eq. (21), and $\beta_\omega=\omega/\omega_n$. It is reminded that, for a linear viscous damping system,

$\left|\boldsymbol{X}(j\omega)\right|$ is represented in the same form as Eq. (37) and the $\left|\ddot{\boldsymbol{X}}_a(j\omega)\right|$ and $\angle\boldsymbol{X}(j\omega)$ are written as

$$\left|\ddot{\boldsymbol{X}}_a(j\omega)\right| = \frac{\sqrt{1+4\beta_\omega^2\xi^2}}{\sqrt{(1-\beta_\omega^2)^2+4\beta_\omega^2\xi^2}} \tag{40}$$

and $$\angle\boldsymbol{X}(j\omega) = \tan^{-1}\frac{2\beta_\omega\xi}{1-\beta_\omega^2} \tag{41}$$

Therefore, a linear viscous damping and a complex stiffness (or complex damping) system will have nearly identical magnitude of displacement responses when the damping ratio of the linear viscous damping system is estimated by Eq. (21) and the value of $\eta$ is used in the complex stiffness system. As indicated by Eqs. (38, 39) and Eqs. (40, 41), the values of $\left|\ddot{\boldsymbol{X}}_a(j\omega)\right|$ and $\angle\boldsymbol{X}(j\omega)$ estimated by the complex stiffness model are different from those estimated by the linear viscous damping model, especially when the value of the damping ratio becomes large. If the damping ratio or loss factor is so small that the numerator of $\left|\ddot{\boldsymbol{X}}_a(j\omega)\right|$ in Eq. (40) approaches 1.0, the displacement and absolute acceleration responses of both models are nearly identical. This means that under low damping conditions, a linear viscous damping model is equivalent to a complex stiffness model for predicting the dynamic response of viscoelastically damped systems. However, there is still a finite difference between the phase angles predicted by Eq. (39) and by Eq. (41).

## 2. Seismic Response

In order to explore the differences in seismic structural responses between a complex stiffness system and a linear viscous damping system, the response spectra of both systems subjected to the El Centro NS-direction earthquake excitation are compared. The required VE dampers are designed based on the MSE1 method for the specified design damping ratios.

From the derivation of the MSE1 method, the assumption of proportional damping is implied in Eq. (6). Therefore, the damping coefficient matrix is formed by the Rayleigh damping model (Clough and Penzien 1993, Chopra 1995) in this study, and the equation of motion is

$$\boldsymbol{M}\ddot{\boldsymbol{x}} + \boldsymbol{C}_{eq}\dot{\boldsymbol{x}} + (\boldsymbol{K}_{VR} + \boldsymbol{K}_0)\boldsymbol{x} = -\boldsymbol{M}\boldsymbol{E}\ddot{\boldsymbol{u}}_g \tag{42}$$

in which $\boldsymbol{C}_{eq}$ is the damping coefficient matrix and the column vector, $\boldsymbol{E}$, is the excitation distribution vector composed of zeros and ones. The structural response can be determined either by the step-by-step integration technique in the time domain or by the discrete Fourier transform method in the frequency domain.

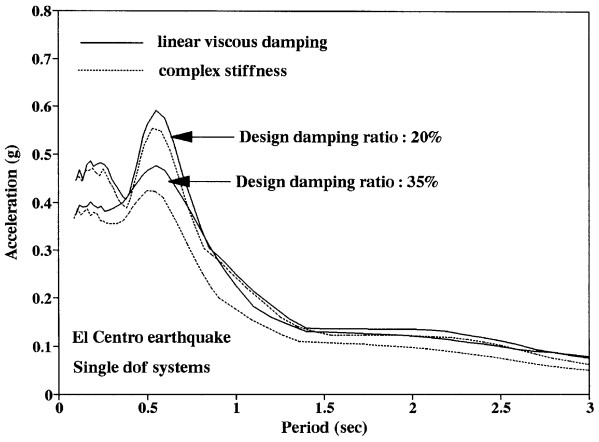


(a)

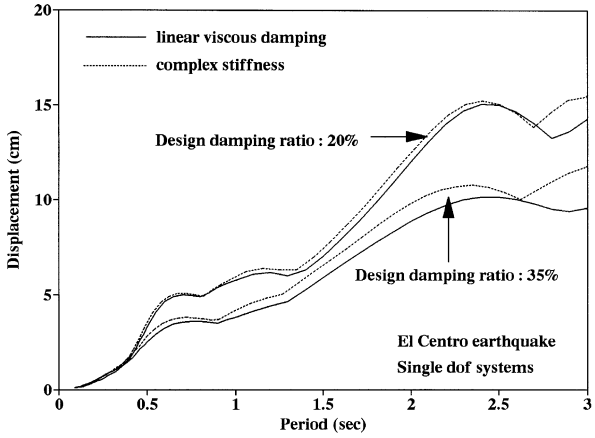


(b)

Fig. 5 (a) Peak acceleration response under the El Centro earthquake excitation (SDOF systems); (b) Peak displacement response under the El Centro earthquake excitation (SDOF systems)

While for the complex stiffness system, instead of forming the damping coefficient matrix, the structural response can be calculated directly in the time domain (Inaudi and Makris 1996) or the frequency domain (Inaudi and Kelly 1995, Aprile *et al.* 1997, Chang *et al.* 1998b). For simplicity, the structural responses of both systems are calculated by the discrete Fourier transform method and neglecting the temperature rise effect of the VE dampers.

*(i) Proportional damping case*

The proportional damping case is illustrated by a SDOF system with added VE dampers. Two selected values of design damping ratios are 20% and 35% corresponding to a medium and a high damping case, respectively. When the VE dampers are designed by the MSE1 method for these two specified damping ratios, the damping ratios predicted by the MSE2 method are 18.9%and 30.0%, respectively.

**Table 1. Predicted modal damping ratios of the non-proportionally damped system**

| | MSE1 method | | MSE3 method | |
|---|---|---|---|---|
| 1st mode | 20% | 35% | 19.0% | 28.7% |
| 2nd mode | 10.7% | 16.5% | 10.9% | 17.4% |

The response spectra of both the linear viscous damping and complex stiffness systems are shown in Figs. 5(a) and 5(b), where the undamped natural period ranges from 0.1 to 3 seconds.

As shown in Fig. 5(b) and indicated by Eq. (37), the displacement response of the linear viscous damping system is generally smaller than that of the complex damping system because the damping ratio predicted by the MSE1 method is larger than that estimated by the MSE2 method. However, since there is an additional term, $4\beta_\omega^2\xi^2$, in the numerator of Eq. (40), the acceleration response predicted by the linear viscous damping system is regularly larger than that predicted by the complex damping system as displayed in Fig. 5(a), especially for the high damping case. Moreover, Fig. 5(a) shows that the benefit of increasing damping is more significant for the complex stiffness system than for the linear viscous damping system, as implied by Eqs. (38) and (40).

From the observation stated above, it is realized that as the damping ratio increases the structural response predicted by the linear viscous damping system, of which the damping ratio is estimated by the MSE1 method, may overestimate the acceleration response and underestimate the displacement response as compared to those predicted by the complex stiffness system.

*(ii) Non-proportional damping case*

For the same 2DOF non-proportionally damped building model described earlier, the design damping ratio, which is now referred to as the first modal damping ratio, is likewise equal to 20% and 35%, respectively, for the moderate and high damping cases. The modal damping ratios predicted by the MSE1 method for the linear viscous damping model and the MSE3 method for the complex stiffness model are listed in Table 1. It should be noted that those values estimated by the MSE3 method should be substituted into Eq. (21) to get the real damping ratios of the non-proportional damping system.

The responses of this non-proportionally damped system are presented in Figs. 6(a) to 6(d). From Figs. 6(a) and 6(b), it is noted that, the increase of damping ratio effectively reduces the acceleration response of the top floor throughout the whole spectral periods. It is, however, only effective within the region of peak spectral response for the lower floor. The top floor acceleration predicted by the complex stiffness system is somewhat larger than that predicted by the linear viscous damping system, while the lower floor acceleration predicted by the complex stiffness system is obviously smaller than that predicted by the linear viscous damping system.

The difference between both models in the displacement response of the top floor is more significant than in that of the lower floor, as displayed in Figs. 6(c) and 6(d). As mentioned earlier, the discrepancy for the displacement response of both systems mainly results from different damping ratios for these two systems. The difference in the top floor accelerations is much smaller than in the lower floor, while in the displacement response, the result is reversed.

From the investigation described above, it is realized that a linear viscous damping system incorporated with the MSE1 method may overestimate the acceleration response of lower stories but underestimate the displacement response of top stories when compared to the responses predicted by the complex stiffness system.

## IV. SUMMARY AND CONCLUSIONS

In this study, the effect of the assumptions made in the modal strain energy method (MSE1) (Johnson and Kienholz 1982) on the prediction of modal damping ratio is first investigated. Modified formulations of the modal strain energy method for a proportionally damped system (MSE2) and a non-proportionally damped system (MSE3) are derived. Analytical results indicate that the difference between the MSE1 and MSE2 methods becomes significant when the damping ratio is larger than 20%. Likewise, for the illustrated non-proportionally damped 2DOF system, the effect of imaginary mode shapes on the MSE1 can be neglected when the damping ratio is smaller than 20%. Otherwise, the MSE1 method may overestimate the modal damping ratio without considering the effect of imaginary mode shapes.

In addition, from the comparison between the structural responses of a linear viscous damping model incorporated with the MSE1 method and a complex stiffness model, it is found that the dynamic behavior of a complex stiffness system can be approximated by a linear viscous damping system incorporated with the MSE1 method when the design damping ratio is below 20%. As the damping ratio increases, although the displacement response of a complex stiffness system can be approximated by a linear viscous damping system combined with the modified modal strain energy method, the discrepancy of their acceleration responses cannot be

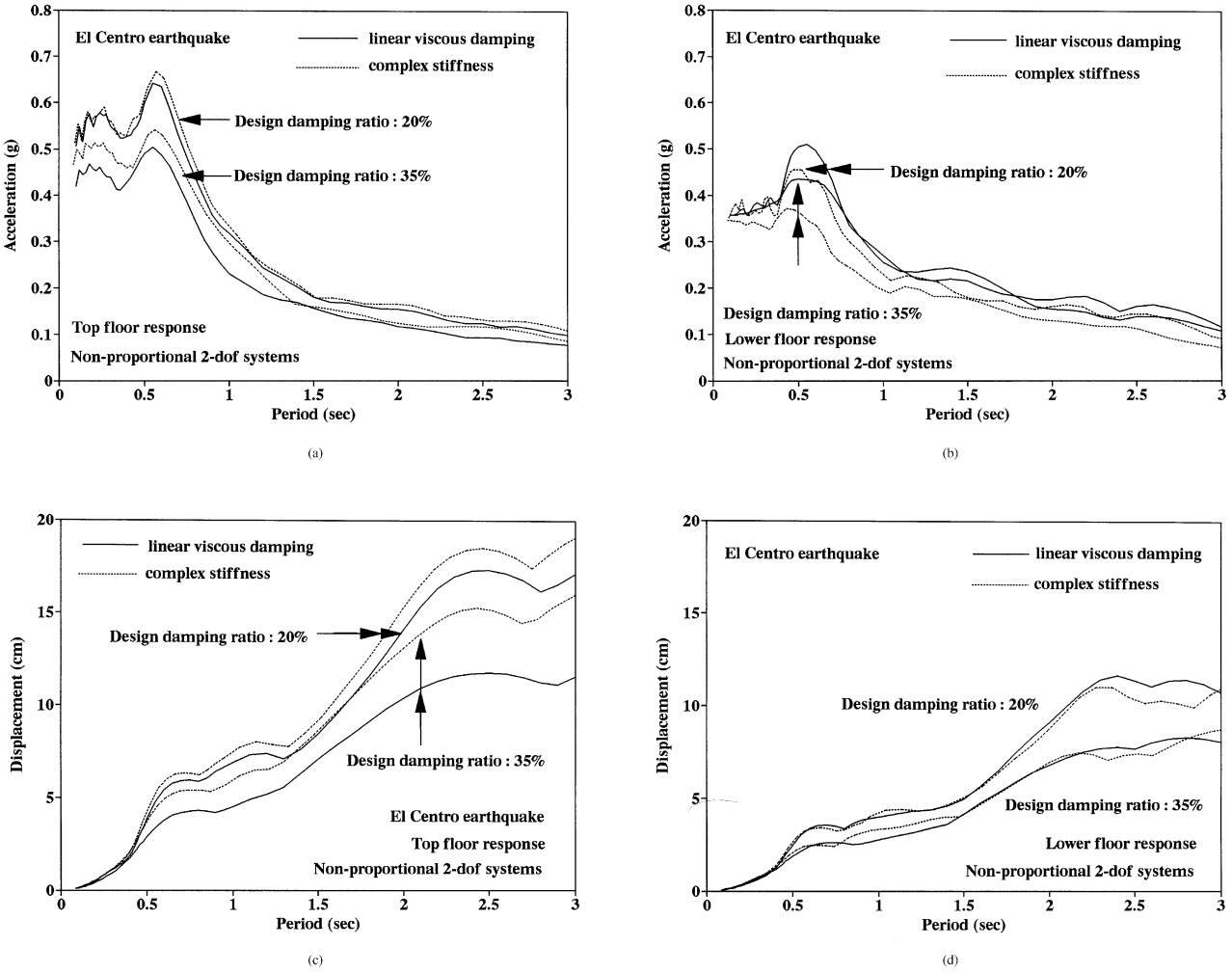


Fig. 6 (a) Peak acceleration response of the top floor under the El Centro earthquake excitation (Non-proportionally damped 2DOF systems); (b) Peak acceleration response of the lower floor under the El Centro earthquake excitation (Non-proportionally damped 2DOF systems); (c) Peak displacement response of the top floor under the El Centro earthquake excitation (Non-proportionally damped 2DOF systems); (d) Peak displacement response of the lower floor under the El Centro earthquake excitation (Non-proportionally damped 2DOF systems)

further reduced by simply modifying the damping ratio. Thus, it may be recommended that, for most engineering applications with design damping ratios smaller than 20%, the conventional linear viscous damping model combined with the MSE1 method will result in solutions in good agreement with that obtained by the more rigorous complex stiffness model.

## ACKNOWLEDGEMENTS

The writers wish to express their sincere appreciation to all the reviewers for their very constructive comments.

## NOMENCLATURE

| | |
|---|---|
| $\boldsymbol{Ceq}$ | damping coefficient matrix |
| $\boldsymbol{E}$ | excitation distribution vector |
| $\boldsymbol{j}$ | unit imaginary number |
| $\boldsymbol{K}_1$ | elastic stiffness matrix of the system |
| $\boldsymbol{K}_2$ | loss stiffness matrix of the system |
| $\boldsymbol{K}_{VI}$ | loss stiffness provided by VE dampers, |
| $\boldsymbol{K}_{VR}$ | storage stiffness provided by VE dampers |
| $\boldsymbol{K}_0$ | elastic stiffness of the primary system |
| $k_1', k_1''$ | storage and loss stiffness of the bottom story |
| $k_2', k_2''$ | storage and loss stiffness of the top story |
| $k_1$ | real part of the complex stiffness of the SDOF system |
| $\boldsymbol{M}$ | mass matrix of the system |
| $m_1, m_2$ | floor mass of the bottom and the top story |
| $R_s$ | elastic stiffness ratio of the 2DOF model |

| | |
|---|---|
| $\boldsymbol{X}(j\omega)$ | displacement vector in the frequency domain |
| $\ddot{\boldsymbol{X}}_a(j\omega)$ | frequency response of the absolute acceleration |
| $\ddot{\boldsymbol{X}}_g(j\omega)$ | Fourier transform of the input acceleration |
| $\lvert\boldsymbol{X}(j\omega)\rvert$ | magnitade of the frequency response of displacement |
| $\lvert\ddot{\boldsymbol{X}}_a(j\omega)\rvert$ | magnitude of the frequency response of acceleration |
| $\angle\boldsymbol{X}(j\omega)$ | phase angle of the displacement response |
| $\boldsymbol{x}$ | displacement vector in the time domain |
| $\ddot{u}_g$ | input excitation vector in the time domain |
| $\alpha$ | real part of the eigenvalue |
| $\beta$ | imaginary part of the eigenvalue |
| $\beta_\omega$ | frequency ratio |
| $\phi_i^*$ | the $i$-th complex mode shape |
| $\phi_R$, $\phi_I$ | real and imaginary part of the complex mode shape |
| $\phi_{1r}$, $\phi_{1i}$ | real and imaginary part of the modal amplitude at the first floor |
| $\gamma$ | mass ratio of the 2DOF model |
| $\eta$ | modal loss factor in the MSE1 method |
| $\eta_V$ | loss factor of VE dampers |
| $\eta_1$, $\eta_2$ | loss factor of the bottom and the top story |
| $\lambda_i^{*2}$ | the $i$-th complex eigenvalue |
| $\lambda$ | undamped modal frequency from the MSE1 method |
| $2\theta$ | phase angle between the force and displacement |
| $\omega_n$ | undamped modal frequency of the viscous damping system |
| $\omega_d$ | undamped natural frequency of the complex stiffness system |
| $\xi$ | modal damping ratio |

## REFERENCES


1. Aprile, A., Inaudi, J.A., and Kelly, J.M., 1997, "Evolutionary Model of Viscoelastic Dampers for Structural Applications," *Journal of Engineering Mechanics, ASCE*, Vol. 123, No. 6, pp. 551-560.
2. Chang, K.C., Lai, M.L., Soong, T.T., Oh, S.T., Hao, D.S., and Yeh, Y.C., 1993, "Seismic Behavior And Design Guidelines for Steel Frame Structures with Added Viscoelastic Dampers." *Technical Report*, NCEER-93-0009, Civil Eng. Dept., State University of New York, Buffalo, NY 14260.
3. Chang, K.C., Soong, T.T., Oh, S.T., and Lai, M.L., 1995, "Seismic Behavior of Steel Frame with Added Viscoelastic Dampers," *Journal of Structural Engineering, ASCE*, Vol. 121, No. 10, pp. 1418-1426.
4. Chang, K.C., Chen S.J., and Lai, M.L., 1996, "Inelastic Behavior of Steel Frames with Added Viscoelastic Dampers," *Journal of Structural Engineering, ASCE*, Vol. 122, No. 10, pp. 1178-1186.
5. Chang, K.C., Lin, Y.Y., and Lai, M.L., 1998a, "Seismic Analysis And Design of Structures with Viscoelastic Dampers," *Journal of Earthquake Technology*, ISET, in press.
6. Chang, K.C., Tsai, M.H., Chang, Y.H., and Lai, M.L., 1998b, "Temperature Rise Effect of Viscoelastically Damped Structures under Strong Earthquake Ground Motions," *Proceedings of the Sixth U.S. National Conference on Earthquake Engineering*, May 31-June 4, Seattle, Washington, U.S., paper No. 217.
7. Chopra, A.K., 1995, *Dynamics of Structures, Theory and Applications to Earthquake Engineering*, Prentice-Hall, Englewood Cliffs, New Jersey.
8. Inaudi, J.A., and Makris, N., 1996, "Time-domain Analysis of Linear Hysteretic Damping," *Earthquake Engineering and Structural Dynamics*, Vol. 25, pp. 529-545.
9. Inaudi, J.A., and Kelly, J.M., 1995, "Linear Hysteretic Damping And The Hilbert Transform," *Journal of Engineering Mechanics, ASCE*, Vol. 121, No. 5, pp. 626-632.
10. Johnson, C.D., and Kienholz, D.A., 1982, "Finite Element Prediction of Damping in Structures with Constrained Viscoelastic Layers," *AIAA Journal*, Vol. 20, No. 9, pp. 1284-1290.
11. Myklestad, N.O., 1952, "The Concept of Complex Damping," *Journal of Applied Mechanics, ASME Transactions*, Vol. 19, September, pp. 284-286.
12. Shen, K.L., Soong, T.T., Chang, K.C., and Lai, M.L., 1995, "Seismic Behavior of A 1/3 Scale RC Frame with Added Viscoelastic Dampers," *Engineering Structures*, Vol. 17, No. 5, pp. 372-380.
13. Zambrano, A., Inaudi, J.A., and Kelly, J.M. 1996, "Modal Coupling And Accuracy of Modal Strain Energy Method," *Journal of Engineering Mechanics, ASCE*, Vol. 122, No. 7, pp. 603-612.


***Manuscript Received: Apr. 12, 2000***
***Revision Received: Jun. 27, 2000***
***and Accepted: Sep. 25, 2000***

# 模態應變能法在黏彈性阻尼結構之應用研究

蔡孟豪　張國鎮

國立台灣大學土木工程學系

**摘　要**

由過去許多試驗與研究顯示，模態應變能法可用來估計加黏彈性阻尼器結構的振態耗損因子或振態阻尼比。然而，在模態應變能法的推演過程中隱含了幾個假設，例如：直接以特徵值的虛部與實部之比值當作振態耗損因子，以及忽略了結構物虛部振形之影響等等。本文將針對上述兩個假設對模態應變能法所估計的阻尼比之影響進行探討，推導不含有該二個假設之模態應變能法。再者，則從複數勁度系統與黏滯阻尼系統兩者的地震反應，比較兩種不同的黏彈性阻尼結構模型之異同，其中黏滯阻尼系統的振態阻尼比乃是從模態應變能法估計而來。研究結果顯示，當阻尼比小於20%時，兩個不同的分析模型會有相近的結構反應。從文中所採用的非比例阻尼系統之地震反應顯示，在阻尼比小於20%的情況下，虛部振形對模態應變能法的影響也可以忽略不計。因此，對於一般設計阻尼比大多小於20%的工程應用範圍，採用黏滯阻尼模型與模態應變能法所得之黏彈性阻尼結構反應，與利用較嚴謹的複數勁度模型之分析結果相近。

關鍵詞：模態應變能法，黏彈性阻尼結構，振態阻尼比。